On the role of post-CCVD synthetic impurities, functional groups and functionalization-based oxidation debris on carbon nanotubes

R. Puskás[1], A. Sápi[1], Á. Kukovecz[1,2], Z. Kónya[1,3 *]

[1] *Department of Applied and Environmental Chemistry, University of Szeged, Rerrich Béla tér 1., H-6720 Szeged, Hungary*

[2] *MTA-SZTE "Lendület" Porous Nanocomposites Research Group, Rerrich Béla tér 1., H-6720 Szeged, Hungary*

[3] *MTA-SZTE Reaction Kinetics and Surface Chemistry Research Group, Rerrich Béla tér 1., H-6720 Szeged, Hungary*

Abstract

A new method has been developed to separately study the effects of (i) impurities resulting from the catalytic chemical vapor deposition synthesis itself, (ii) the attached functional groups and (iii) the oxidation debris on the properties of carboxyl-functionalized multiwall carbon nanotubes (CNTs) by incorporating a Soxhlet-extractor enhanced acetone washing process into the synthesis method. Palladium nanoparticles supported on the carbon nanotubes were investigated in the hydrogenation of cyclohexene to cyclohexane. Despite the fact that the specific surface area and the Pd dispersion were both low, the Pd/CNT catalyst with post-synthetic impurities showed ~20 times higher catalytic activity compared to functional group free, acetone-washed samples. While oxidation debris originating from the functionalization was found to affect both the specific surface area and the G/D ratio obtained from Raman spectra, it had little effect on the size of the supported Pd nanoparticles or catalytic activity. On the other hand, functional groups have significant effect on the catalytic activity without influencing the specific surface area, the G/D ratio or the Pd nanoparticle dispersion.

* Corresponding author. Tel: Email: konya@chem.u-szeged.hu

1. Introduction

Carbon nanotubes (CNT) have been targeted by considerable scientific interest in the past decades, especially in the field of heterogeneous catalysis. Nanoparticles of different types and sizes supported on CNTs were tested in many catalytic reactions, such as hydrogenation, dehydrogenation, and oxidation [1,2,3,4,5,6,7,8,9]. The most common methods of carbon nanotube synthesis are based on the catalytic chemical vapor deposition (CCVD) process. This method can result in amorphous carbon based impurities [10] that may affect the catalytic performance.

The effect of carbon nanotube oxidation on the sorption of both organic and inorganic substances [11,12,13,14,15] the size of supported nanoparticles [16,17] and the length of carbon nanotubes [18,19,20] has also been extensively studied. In the case of nanotube length for example, it has been found that extended oxidation time reduces nanotube length significantly and the most prominent shortening occurs in the first few hours of oxidation. This phenomenon can have several implications on catalytic reactions for example.

Some oxidation techniques can produce oxidation debris on the carbon nanotube surfaces, which can influence chemical and biological properties. This debris forms when the caps and outer layers of nanotubes are attacked by the acid. During intensive oxidation, holes can form in the individual carbon layers and can grow up to a point where they are interconnecting and leave small parts of the outer graphitic layer separate from the main layer. These small oxidized graphene “islands” then get peeled off to either form amorphous content on the surface or be oxidized completely to CO_2 [21,22].

Zhang and co-workers investigated how defects are generated in single walled carbon nanotubes subjected to different oxidants. It has been found that after the initial attack of the oxidant on existing active sites (e.g. -CH, -CH_2 groups, Stone-Wales defects) an electrophilic addition begins at hexatomic-hexatomic boundries producing new active sites or rather, new defects. The authors consider this to be a defect generating step, which is then accompanied by a defect consuming step, where the graphitic structure around existing active sites is destroyed during intense oxidation [23].

The effect of removal of such debris has been studied to some extent [24,25,26,27,28] already. The most common removal methods are based on washing with

aqueous solutions under neutral or basic conditions. However, the basic washing solution can react with the surface carboxylic groups of the carbon nanotubes, while water will not necessarily dissolve all organic residues and consequently, the surface is either altered or not cleaned properly.

We have developed a thorough Soxhlet-extractor washing process with acetone to remove all forms of synthesis and oxidation debris from CNT surfaces. This process allowed us to separately study the effects of post-synthetic (post-CCVD) impurities, wet chemical oxidation-based functional groups and attendant oxidation debris on the various chemical and physical properties of carbon nanotubes. In order to follow these effects, CCVD synthesized multiwall carbon nanotubes have been oxidized in concentrated nitric acid for 4-24 h and washed in acetone using a Soxhlet-extractor. The effects of post-CCVD impurities, functional groups and oxidation debris were followed by altering the order of oxidation and washing steps. The resulting changes in specific surface area and general carbon structure were followed by nitrogen porosimetry and Raman spectroscopy. Finally, the functionalized carbon nanotubes were impregnated with Pd nanoparticles and catalytic hydrogenation of cyclohexene was performed on the Pd/CNT catalysts. The duration of oxidation and the order of washing have highly affected the physical properties of the carbon nanotubes as well as the size of the supported Pd nanoparticles and the catalytic activity, which suggests a complex role of post-CCVD impurities, functional groups and oxidation debris.

2. Experimental

2.1. Sample preparation

Multiwall carbon nanotubes (MWCNT) were prepared in our laboratory by the well-known catalytic chemical vapor deposition (CCVD) method described elsewhere [29]. The as-prepared MWCNT samples were modified in different washing and functionalization processes as described as follows.

The oxidation of MWCNTs was performed by thermally assisted oxidation, where fixed amounts (4-4 g) of MWCNTs were refluxed in cc. HNO_3 solution (500 ml, 65 wt%) for 0, 4, 8, 12, 16, 20 and 24 h to generate oxygen-containing surface functional

groups. The products were washed with distilled water to neutral pH and dried overnight at 80 °C in air.

In one series, 4-4 g of functionalized carbon nanotubes with different oxidation durations were washed with 500 ml of acetone in a Soxhlet-extractor for 48 h and dried again overnight at 80 °C. These samples are denoted as "After Washed" carbon nanotubes (CNT-AW).

In another series, the functionalized carbon nanotubes were washed with the same procedure as described above before the oxidation-assisted functionalization. These samples are denoted as "Before Washed" carbon nanotubes (CNT-BW).

The effect of washing was compared to functionalized carbon nanotubes not subjected to any washing process. These samples are denoted as "Not Washed" carbon nanotubes (CNT-NW).

Palladium nanoparticles were impregnated onto the surface of the different MWCNT samples by the well-known wet impregnation method using toluene as the medium and palladium(II)-acetate (Sigma-Aldrich) as the palladium source. In a typical procedure, 22 mg of $Pd(II)(ac)_2$ was dissolved in 100 ml toluene, then 200 mg CNT was added to the solution and the mixture was sonicated for 15 min in an ultrasonic bath (80 W) and stirred for 24 h at room temperature. The samples were then centrifuged at 3200 rpm and dried in air at 80 °C overnight. The as-prepared samples were finally annealed at 185 °C for 2 h followed by 380 °C for 1 h in nitrogen atmosphere, where the metal salt completely decomposed to yield metallic Pd nanoparticles on the carbon nanotube surface [30]. Pd-impregnated samples are denoted as Pd-CNT-AW, Pd-CNT-BW and Pd-CNT-NW. A simplified graphical schematic is presented in Figure 1 to help better understand the changes made by various preparation steps on the surface environment of carbon nanotubes.

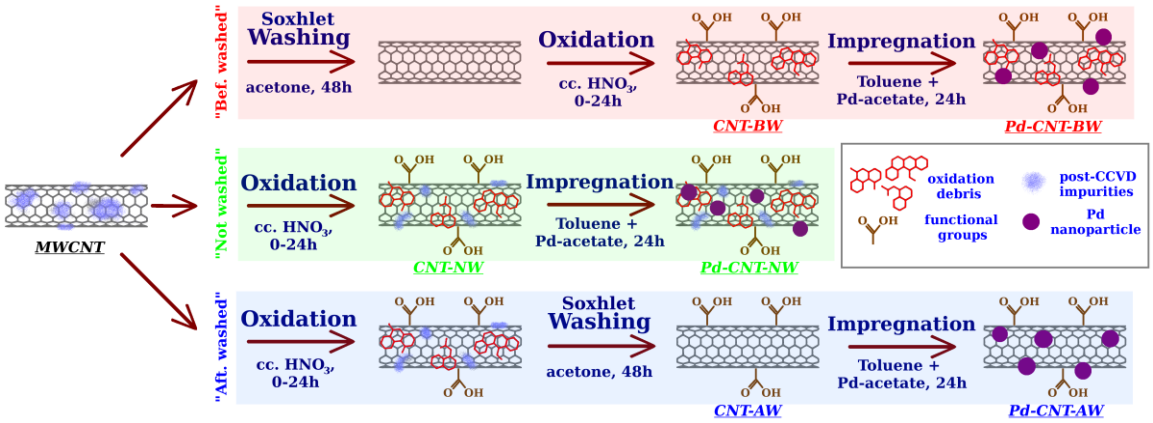

Figure 1: A graphical overview of the effects of various sample preparation steps on the surface environment of carbon nanotubes

2.2. Sample characterization

Raman spectra were collected at 4 cm^{-1} resolution for 3 min using a Thermo Scientific Raman DXR microscope with a 532 nm laser excitation operated at 5 mW. Nitrogen adsorption data were collected on a Quantachrome NOVA 3200 instrument. All samples were degassed for 1.5 h in vacuum at 380 °C before measurement.

Transmission electron microscopy (TEM) was performed using a FEI Tecnai G^2 20 X-TWIN microscope with a tungsten cathode operated at 200 kV. Powder X-ray diffraction (XRD) patterns were collected in a Rigaku Miniflex II desktop diffractometer using Cu K_α irradiation at a scan speed of 4°·min^{-1} and 0.25 °·min^{-1} in the ranges 2θ = 5-90° and 2θ = 35-50°, respectively.

To determine the Pd concentration, several Energy Dispersive X-ray Spectroscopy (EDS) measurements were conducted on each sample with a Röntec QX2 detector mounted on a Hitachi S-4700 scanning electron microscope.

Catalytic hydrogenation of cyclohexene to cyclohexane was performed in a continuous flow reactor system at 40 °C, where the ratio of cyclohexene:hydrogen:nitrogen was 1:10:90 with a total flow rate of 101 ml·min^{-1} at 1 bar. Product analysis was performed on-line with an Agilent 6820 gas chromatograph using a flame ionization detector.

3. Results and discussion

3.1. Raman spectroscopy

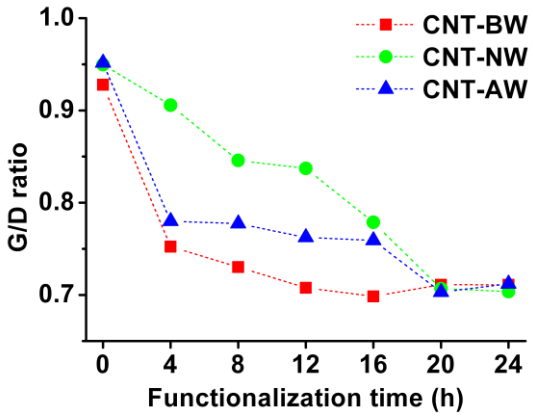

Figure 2: Raman G/D band ratios of multiwall carbon nanotube samples after different functionalization durations (4-24 h) in the case of "Non Washed", "Before Washed" and "After Washed" samples (lines are guide to the eye). The G/D ratio of "Non washed" samples decreases whilst samples washed before or after oxidation show different changes. These differences originate from the various effects of post-CCVD impurities, surface functional groups and oxidation debris on the Raman spectra. While post-CCVD impurities and surface functional groups were not found to severely affect G/D ratios, oxidation debris had notable altering effect.

Raman spectra were collected on all three sample series (CNT-AW, CNT-BW and CNT-NW samples). Raman spectra are presented in Figure S3. The intensity ratio of the well-known Raman D and G bands at ~1349 and 1586 cm^{-1}, respectively, was examined to reveal possible structural changes of carbon nanotubes with the functionalization time (Figure 2). The graphitic or G band is attributed to the tangential lattice vibrations of sp^2 bonded carbon atoms. Meanwhile, the intensity of the disorder induced D band is generally associated with the amount of defects, or more precisely the amount of sp^3 hybridized phonon scattering sites.

In case of CNT-NW, the G/D ratio decreased from 0.95 to 0.9 after 4 h of oxidation then further to the final value of 0.71 (25% drop) in the next 20 h. This is in agreement with previous studies where nitric acid was used for the oxidation of carbon nanotubes [22]. Interestingly, both the CNT-AW and the CNT-BW series show ~20% decrease in G/D ratio after 4 h oxidation time already. Values of CNT-AW's are slowly decreasing from 0.78 to 0.76 from 4 h to 16 h, reaching 0.70 at even longer functionalization times. After the ~20% drop in the first 4 hours, the CNT-BW samples show a slow G/D ratio decrease from 0.75 to 0.70 between 4-16. The G/D ratio is independent of the washing process if functionalization is performed for longer than 20 h.

A clearly distinguishable G/D ratio decrease is visible in both the CNT-NW and the CNT-BW sample series between 4 and 16 h of oxidation. This drop can be attributed to the continuously formed oxidation debris and functional groups created by the nitric acid oxidation, as no washing process was used after functionalization in these series.

However, the G/D ratios of the CNT-NW are always higher than those of the CNT-BW samples, which can be attributed to the application of the washing process before oxidation in the case of CNT-BW. As washing applied before oxidation can only remove already present impurities, namely the post-CCVD ones, the higher G/D values of CNT-NW compared to CNT-BW indicate that post-CCVD impurities have a significant effect on the oxidation process.

Interestingly, the washing process did not seem to alter G/D ratios of non-functionalized, 0 h samples, which indicates that post-CCVD impurities resulting directly from the carbon nanotube synthesis are only present in small quantities. Nevertheless, their amount is enough to alter surface properties as will be evidenced by nitrogen adsorption measurements later.

As discussed previously, the steadily decreasing G/D ratio in the CNT-NW series could probably be attributed to the formation of both oxidation debris and functional groups. On the other hand, washing the nanotubes after oxidation alters G/D ratios considerably, as evidenced by the CNT-AW samples. The G/D ratio of CNT-AW samples exhibits a sudden drop at 4 h of oxidation followed by insignificantly small further changes up until 16 h. This phenomenon must be caused by the washing process: oxidation debris is removed regardless of the functionalization time, leaving only functional groups unaffected by washing on the surface. These groups do not seem alter the G/D ratio of the nanotubes.

G/D intensity ratios of CNT-AW samples are slightly higher in the 4-20 h functionalization time range than those of the corresponding CNT-BW series. This is because the samples of the CNT-AW series were washed only after the oxidation process, thus post-CCVD impurities were still present on the surface of nanotubes during the acidic treatment. Since the graphitic structure of nanotubes is less prone to oxidation then the structurally amorphous impurities, it can be assumed that these post-CCVD impurities are preferentially consumed by the nitric acid, thus exhibiting a shielding effect for

nanotube walls. This resulted in a slightly smaller number of defective sites on the walls of the carbon nanotubes compared to CNT-BW samples, where no impurities were present at the time of oxidation and the nitric acid attack could be fully directed at the CNT walls.

Samples with oxidation times higher than 20 h show virtually identical G/D ratios, which could imply that at this stage the concurring defect-generating and defect-consuming processes have reached equilibrium. These results thus indicate, that while oxidation-related debris greatly affects the detected Raman signal, post-CCVD impurities and anchored functional groups barely alter the obtained spectra even though they can have major impact on other attributes of the samples.

3.2. Nitrogen gas adsorption

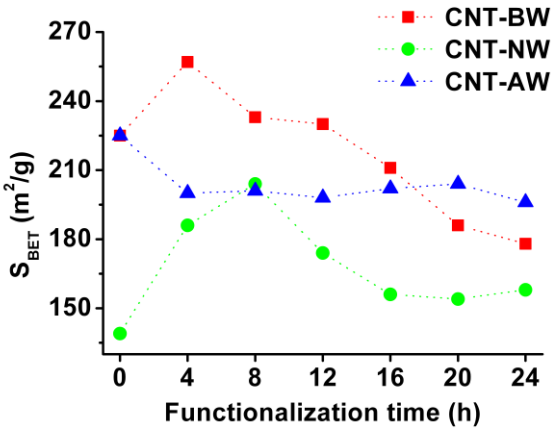

Figure 3: Specific surface area of carbon nanotubes subjected to different washing processes as a function of the oxidation time. Lines are guides for the eye only. The specific surface area of carbon nanotubes washed with acetone after functionalization does not change with functionalization time. This evidences the formation of oxidation debris that can be removed by the washing process.

Nitrogen gas adsorption isotherms were measured for all carbon nanotube samples. The specific surface area (S_{BET}) was calculated using the well-known Brunauer-Emmett-Teller (BET) method. By inspecting S_{BET} data plotted in Figure 3, clear and significant effects of the functionalization time and the acetone washing process are visible.

In case of CNT-BW samples, S_{BET} value rises from 225 $m^2 \cdot g^{-1}$ to 257 $m^2 \cdot g^{-1}$ at 4 h of oxidation, then it shows a steady drop up to 24 h functionalization where it reaches 178 $m^2 \cdot g^{-1}$.

The initial S_{BET} value of the CNT-NW sample is 140 $m^2 \cdot g^{-1}$, then it increases to 205 $m^2 \cdot g^{-1}$ after 8 h functionalization and decreases again to 155 $m^2 \cdot g^{-1}$ by 16 h. There is no significant change in specific surface area after 16 h of functionalization for CNT-NW samples.

CNT-AW samples do not display the tendencies showed by the CNT-BW and CNT-NW series. Rather, their S_{BET} of 225 $m^2 \cdot g^{-1}$ drops to 200 $m^2 \cdot g^{-1}$ at 4 h and remains fairly constant at this value at longer functionalization times.

The sudden rise of S_{BET} value on samples CNT-BW and CNT-NW can be attributed to the opening of nanotube endings by the oxidation of the caps in the first few hours of oxidation. The higher C-C bonding curvature and pentagon concentration make these sites more prone to oxidation [31]. The following steady drop in the specific surface area when using higher functionalization times can be assigned to the formation of oxidation debris composed mainly of peeled off oxidized graphene “islands” forming amorphous carbon [21,32] that can make adsorption sites located in interstitial and intratube pores partly inaccessible for nitrogen [33].

The presence of post-CCVD contamination is evidenced by the difference in S_{BET} values between CNT-BW and CNT-NW non-oxidized samples, as the washing process with acetone resulted in an almost 40 % increase in S_{BET} from 140 $m^2 \cdot g^{-1}$ to 225 $m^2 \cdot g^{-1}$. It is important to note here, that while washing did not significantly alter the Raman spectra, it did cause a significant change in the specific surface area of non-functionalized samples. This supports the assumption that post-CCVD contamination can greatly alter the surface properties of carbon nanotubes. The difference in specific surface area values between CNT-BW and CNT-NW samples does not disappear at longer functionalization times. This parallel behavior suggests similar defect origin for functionalization times longer than ~8 h, namely, the oxidation debris formed during the functionalization processes. The slight shift of peak maximum position to longer oxidation times of CNT-NW samples compared to CNT-BW samples is due to the presence of post-CCVD contamination, which could reduce the speed of the cap opening.

The fairly constant specific surface area value of ~200 $m^2 \cdot g^{-1}$ measured for all oxidized CNT-AW samples is the result of the removal of oxidation debris by the washing process. This means that the oxidative treatment and the resulting functional groups do not seriously alter the specific surface area of the nanotubes themselves, not even after prolonged exposure to the acidic treatment. Rather, differences in the S_{BET} values are related to the blockage of various pores and adsorption sites by the debris formed during the oxidation process. Results for non-oxidized washed samples also indicate that post-CCVD impurities greatly alter S_{BET} values even in small quantities, even though they are not detectable by Raman spectroscopy.

3.3. Transmission electron microscopy

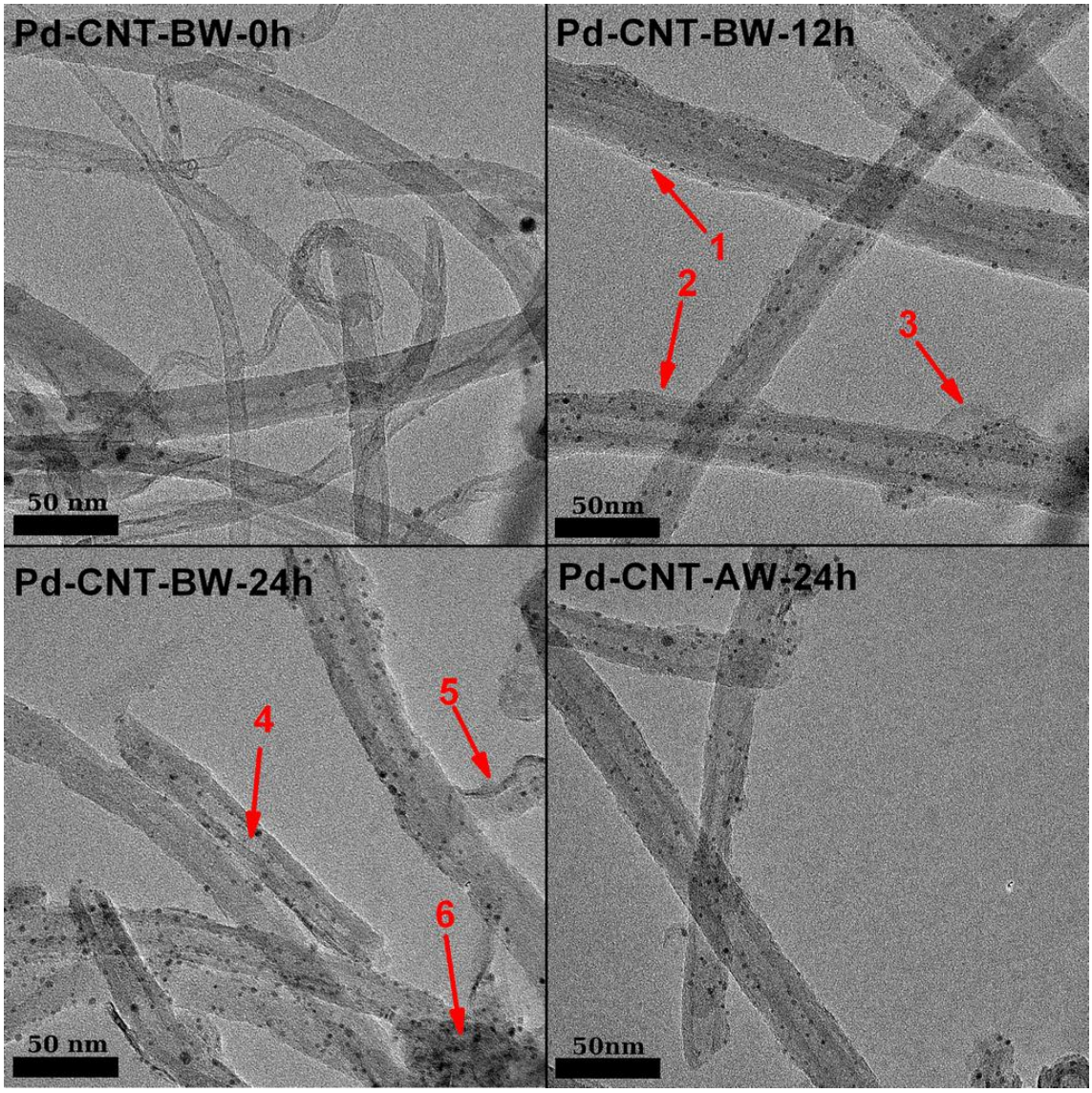

Figure 4: TEM micrographs of Pd/CNT samples from the "Before Washed" series with nanotube supports oxidized for 0, 12 and 24 h. Numbered arrows highlight distinct features of oxidized samples, such as surface coverage (1,2), loose layers of CNT (3), short nanotube pieces (4) CNT fragments (5) and amorphous content (6). The surface of "After Washed" nanotube sample oxidized for 24 h contains no debris or other contaminants.

The structure of carbon nanotubes and supported Pd nanoparticles was examined by transmission electron microscopy (TEM). TEM micrographs of carbon nanotube supported Pd nanoparticles can be found in Figure 4 and S1. All particles are evenly dispersed on the surface of the carbon nanotubes. Non-supported particles are not observable. Pd particle diameters were manually determined for each sample by

measuring at least 200 particles per sample. Calculated mean diameters and standard deviations are tabulated in Table 1.

Table 1: Average diameter and standard deviation of supported Pd nanoparticles.

Oxidation time (h)	Particle diameter (nm)		
	Pd-CNT-BW	Pd-CNT-NW	Pd-CNT-AW
0	2.7 ± 0.8	4.8 ± 2.3	2.7 ± 0.8
4	2.3 ± 0.4	3.6 ± 1.2	2.7 ± 0.6
8	2.3 ± 0.4	2.9 ± 0.9	2.7 ± 0.7
12	2.2 ± 0.4	2.3 ± 0.5	2.8 ± 0.9
16	2.3 ± 0.5	2.2 ± 0.5	2.9 ± 0.9
20	2.3 ± 0.7	2.3 ± 0.6	2.8 ± 0.6
24	2.6 ± 0.8	2.2 ± 0.5	2.9 ± 0.6

The formation of metallic Pd was also confirmed by powder XRD measurements, where peaks characteristic for fcc Pd (111) and Pd (200) reflections were detected on all Pd modified samples at d-spacing values of 2.24 and 1.93 Å, respectively. Calculation of crystallite sizes with Scherrer's equation was not possible due to the pronounced peak broadening typical in this particle size regime. XRD patterns are presented in the supplementary information (Figure S2).

The average Pd particle diameter was 4.8 nm for Pd-CNT-NW samples without functionalization. This value decreased to 3.6 nm at 4 h, 2.9 nm at 8 h and reached 2.3 nm at 12 h, then remained fairly constant up to 24 h functionalization time. The Pd-CNT-BW and Pd-CNT-AW samples featured an average particle diameter of 2.4 nm and 2.8 nm, respectively independent of the functionalization duration. The standard deviation of the particle diameter was below 1 nm for most of the samples. However, Pd nanoparticles supported on non-functionalized carbon nanotubes showed slightly higher standard deviation of 0.8-2.3 nm.

As evidenced by the micrograph of the acetone-washed, non-oxidized (0h) CNT sample (Figure 4), the surface of the nanotubes is completely intact. No contamination of any sort is visible on the surface. However, after 12 h of oxidation evidences of surface coverage (Arrows 1 and 2, Fig. 4) and some loose layers (Arrow 3, Fig. 4) become

visible, which are most probably the oxidation debris formed during functionalization. After 24 h of oxidation the results of the extensive acid treatment: amorphous carbon content (Arrow 6, Fig. 4) and CNT fragments (Arrow 5, Fig. 4) appear on the surface of the carbon nanotubes. Moreover, nanotubes could break up into shorter pieces during prolonged oxidation as evidenced by the Pd-CNT-BW-24h sample (Arrow 4, Fig. 4). No surface contamination can be identified on the Pd-CNT-AW-24h sample, which provides independent verification for the successful removal of oxidation debris by the Soxhlet-extractor washing.

In the case of CNT-NW samples, oxidation times yielded Pd nanoparticle diameters similar to our earlier observations [16]. The size of the Pd nanoparticles supported on CNT-BW and CNT-AW series of carbon nanotubes seem to be entirely insensitive to the functionalization time. It must be noted however, that in case of washed and not washed unfunctionalized samples the mean diameter changed to 2.7 ± 0.8 nm from 4.8 ± 2.3 nm, respectively. This indicates a major change in the carbon nanotube surface environment due the removal of post-CCVD impurities during the Soxhlet-extractor washing process.

Although the changes in Raman G/D intensity ratios were very similar between the CNT-BW and CNT-AW series, the corresponding S_{BET} values exhibit considerable differences. Let us now clarify that the dissimilarity revealed by the nitrogen sorption studies does not contradict the previously found Raman similarities between the washed samples, rather, it can help us understand how the washing process alters the environment of the carbon nanotube surfaces and which types of carbon species contribute to Raman spectra or alter the size of Pd nanoparticles with functionalization time. Nitrogen sorption data of CNT-BW samples indicate that oxidation debris is formed during extended functionalization, which lowers S_{BET} after 4 h. Post-CCVD impurities influence the nanoparticle size and size distribution as evidenced by the TEM studies of the unfunctionalized samples. The presence of oxidation debris does not seriously alter the size of supported particles. This may be attributed to the fact that oxidation debris does not encompass the available surface of the carbon nanotubes, rather, it accumulates in certain spots like interstitial and intratube pore entrances (nanotube endings). Since nanotubes are impregnated with Pd nanoparticles only after functionalization, the inner

surfaces of the CNTs are available for Pd nanoparticle anchoring during impregnation from the toluene solution of the $Pd(II)(ac)_2$. Oxidation debris does not enter the inner pores of nanotubes, therefore, Pd nanoparticles anchored on the inner walls of nanotubes are simply not affected by the debris. Nanoparticles anchored on the outer walls of nanotubes seem to be equally insensitive to the presence of oxidation debris. These findings suggest that while post-CCVD impurities affect supported Pd nanoparticle size, oxidation debris does not have significant effect on the nanoparticles.

3.4. Cyclohexene hydrogenation

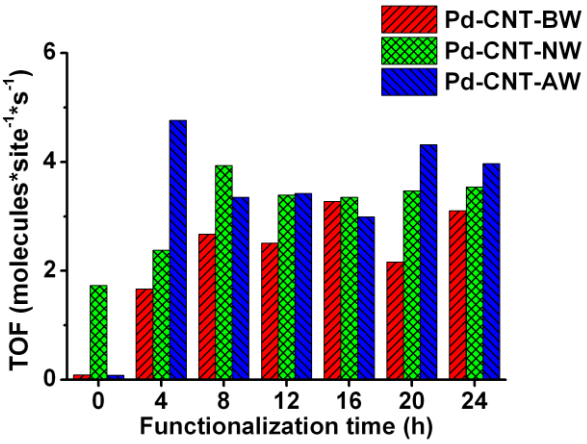

Figure 5: The difference in TOF 10 minutes after the initialization of the catalytic reaction. Catalysts supported on non-oxidized CNTs demonstrate the beneficial effect of post-CCVD impurities on conversion. On the other hand, samples oxidized for 4 h evidence the inhibition effect of oxidation debris as a evidenced by the sudden leap in TOF on "after washed" sample.

Continuous flow catalytic reaction tests were performed on all samples to reveal further details on the effects of functionalization and washing. The hydrogenation of cyclohexene to cyclohexane was monitored and turnover frequencies (TOF) were calculated for all samples after 10 min of reaction time (Figure 5).

In case of CNT-NW samples, a TOF value of 1.7 molecules·site^{-1}·s^{-1} was measured for the unfunctionalized sample, then increased steadily to 2.4 at 4 h and reached 3.9 at 8 h oxidation. No significant changes were observed in the TOF at longer oxidation times.

On the other hand, unfunctionalized Pd-CNT-BW and Pd-CNT-AW samples showed no significant cyclohexene conversion, whereas longer oxidation times resulted

in TOF values comparable or even larger than those of the corresponding Pd-CNT-NW samples. This can be attributed to the increasing amount of polar, oxygen containing functional groups on the surface with the progression of functionalization. Interestingly, acetone-washed, non-oxidized (0 h) samples showed almost negligible TOF values compared to the 1.7 molecules·site^{-1}·s^{-1} value of the non-washed one, which seems to indicate that the presence of post-CCVD impurities has a significant effect on the catalytic activity. On the other hand, CNT-AW and CNT-BW samples oxidized for 4 h exhibited significant hydrogenation activity (1.65 and 4.8 molecules·site^{-1}·s^{-1}, respectively) compared to non-oxidized samples. These results show that the presence of the post-CCVD impurities can inhibit the oxidation process and/or the removal of the oxidation debris can enhance catalytic activity.

Nanotubes oxidized for 8 h or longer show almost identical TOF values for all samples, which suggests that oxidation debris and functional groups do not alter the cyclohexene conversion in these samples as the size of the Pd nanoparticles has not changed with oxidation time in the 8-24 h range. This could be explained by the fact that carbon nanotubes break up into shorter nanotubes during prolonged oxidation [20], thus the shortening of nanotubes reduces transport resistance making the effect of oxidation debris less significant. Moreover, the inner nanotube surfaces are less prone to get covered by oxidation debris because of the narrower entrance diameter of inner nanotube pores compared to intertubular pores of forming CNT agglomerates. This is important, as it is possible for nanoparticles to be anchored in the interior of CNT and therefore, they are less affected by debris. These phenomena can explain why there is no decrease in TOF for CNT-NW and CNT-BW samples despite the fact that the specific surface area tends to decrease for functionalization times longer than 8 h. Consequently, oxidation debris blocks mostly intertube pores in the forming agglomerates, but not necessarily the inner pores of tubes.

Interestingly, despite the fact that cyclohexene hydrogenation can be considered a structure sensitive reaction [34], no significant differences in TOF were found between the washed and non-washed sample series, even though some kind of difference could be expected due to nanoparticle size variation in the non-washed series. This suggests that

surface diffusion and sorption properties of reactants are the main governing factors of reaction rates under such reaction conditions.

4. Conclusion

A new method was devised to study the effects of post-CCVD impurities, functional groups and oxidation debris separately on various properties of carbon nanotubes by incorporating a Soxhlet-extractor enhanced acetone washing process into the standard synthesis method of oxidized carbon nanotubes. It has been found that while the presence of post-CCVD impurities reduced the specific surface area severely from 225 m^2/g to 140 m^2/g in non-oxidized nanotubes, it had a positive effect on cyclohexene hydrogenation TOF: non-washed samples exhibited a value of 2.7 $molecules \cdot site^{-1} \cdot s^{-1}$ compared to the value of ~0.1 $molecules \cdot site^{-1} \cdot s^{-1}$ of acetone washed samples. Post-CCVD impurities also affected supported Pd nanoparticle size heavily, but had little effect on Raman G/D intensity ratios.

Oxidation debris was also found to significantly alter the S_{BET} of carbon nanotubes by blocking intertubular pores, but had little effect on TOF. This phenomenon can be attributed to the shortening of carbon nanotube by prolonged oxidation, which resulted in reduced transport resistance. The presence of oxidation debris has no effect on the size of the supported Pd nanoparticles, but affects Raman G/D intensity ratios.

Functional groups have insignificant effect on the S_{BET} or Raman G/D ratios. Post-CCVD impurities heavily affect S_{BET} but do not change G/D ratios. Unlike post-CCVD impurities, functional groups have no effect on the size of supported Pd nanoparticles.

The above results are summarized in a simple graphical representation in Figure 6, where the effect of individual surface modifying species (post-CCVD impurities, oxidation debris and functional groups) is visually highlighted for various investigated attributes.

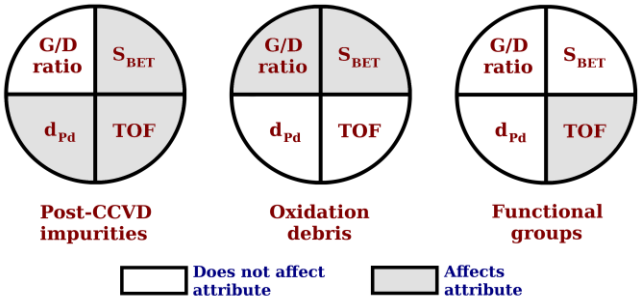

Figure 6: A simple graphical representation of the connections between various attributes of samples and different surface structures (post-CCVD impurities, oxidation debris and functional groups). Tinted areas represent a known effect on the specific attribute by the appropriate surface modifying species, whereas white areas represent a negligible or no effect on an attribute.

These results thus have several implications on the design of materials based on carbon nanotubes for various uses like catalyst supports, adsorbents or sensor materials. Sensors for example heavily rely on adsorption and conductivity, thus the change of surface properties due to the removal oxidation debris and/or post-synthetic impurities under specific environments could seriously alter the sensitivity and selectivity of these materials. Such environments could include repeated usage of such materials in e.g. aqueous solutions of organic solvents, at elevated temperatures or in any other environment that leaves nanotubes intact but not the impurities. These results also call for more careful planning at second generation modification of nanotubes (e.g. amidation, esterification, etc.) as functional groups attached to oxidation debris can simply be removed by extensive washing unlike those attached to the nanotubes themselves.

Acknowledgement

[a]This research was supported by the European Union and the State of Hungary, co-financed by the European Social Fund in the framework of TÁMOP-4.2.4.A/ 2-11/1-2012-0001 ‘National Excellence Program’.

[b]This paper was also supported by the János Bolyai Research Scholarship of the Hungarian Academy of Sciences of SA.

[c]The financial support of the OTKA projects NN 110676 and K 112531 is acknowledged.

References:

[1] Li CH, Yu ZX, Yao KF, Ji SF, Liang J. Nitrobenzene hydrogenation with carbon nanotube-supported platinum catalyst under mild conditions. J Mol Catal A: Chem 2005; 226(1):101-105

[2] Liang XL, Dong X, Lin GD, Zhang HB. Carbon nanotube-supported Pd–ZnO catalyst for hydrogenation of CO2 to methanol. Appl Catal, B 2009; 88(3-4):315-322

[3] Yoon B, Pan HB, Wai CM. Relative Catalytic Activities of Carbon Nanotube-Supported Metallic Nanoparticles for Room-Temperature Hydrogenation of Benzene. J Phys Chem C 2009; 113(4):1520-1525

[4] Liu ZJ, Xu Z, Yuan ZY, Lu D, Chen W, Zhou W. Cyclohexanol dehydrogenation over Co/carbon nanotube catalysts and the effect of promoter K on performance. Catal Lett 2001; 72(3-4):203-206

[5] Wang Y, Shah N, Huggins FE, Huffman GP. Hydrogen Production by Catalytic Dehydrogenation of Tetralin and Decalin Over Stacked Cone Carbon Nanotube-Supported Pt Catalysts. Energy Fuels 2006; 20(6):2612-2615

[6] Peng F, Fu XB, Yu H, Wang HJ. Preparation of carbon nanotube-supported Fe2O3 catalysts and their catalytic activities for ethylbenzene dehydrogenation. New Carbon Mater 2007; 22(3):213-217

[7] Wu G, Xu BQ. Carbon nanotube supported Pt electrodes for methanol oxidation: A comparison between multi- and single-walled carbon nanotubes. J Power Sources 2007; 174(1):148-158

[8] Yang X, Wang W, Qiu J. Aerobic oxidation of alcohols over carbon nanotube-supported Ru catalysts assembled at the interfaces of emulsion droplets. Appl Catal, A 2010; 382(1):131-137

[9] Winjobi O, Zhiyong Z, Liang C, Li W. Carbon nanotube supported platinum–palladium nanoparticles for formic acid oxidation. Electrochim. Acta 2010; 55(13):4217-4221

[10] Biro LP, Khanh NQ, Vertesy Z, Horvath ZE, Osvath Z, Koos A, et al. Catalyst traces and other impurities in chemically purified carbon nanotubes grown by CVD. Mater Sci Eng, C 2002; 19(1-2):9-13

[11] Pyrzynska K, Bystrzejewski M. Comparative study of heavy metal ions sorption onto activated carbon, carbon nanotubes, and carbon-encapsulated magnetic nanoparticles. Colloids Surf, A 2010; 362(1-3):102-109

[12] Ricca A, Bauschlicher CW Jr. The physisorption of CH4 on graphite and on a (9,0) carbon nanotube. Chem Phys 2006; 324():455–458

[13] Wongkoblap A, Do DD, Wang K. Adsorption of polar and non-polar fluids in carbon nanotube bundles: Computer simulation and experimental studies. J Colloid Interface Sci 2009; 331(1):65-76

[14] Horastani ZK, Hashemifar SJ, Sayedi SM, Sheikhi MH. First-principles study of H2adsorption on the pristine and oxidized (8,0) carbon nanotube. Int J Hydrogen Energy 2013; 38(31):13680-13686

[15] Schierz A, Zanker H. Aqueous suspensions of carbon nanotubes: Surface oxidation, colloidal stability and uranium sorption. Environ Pollut 2009; 157(4):1088-1094

[16] Puskas R, Kukovecz Á, Konya Z. Effects of carbon nanotube functionalization on the agglomeration and sintering of supported Pd nanoparticles. Adsorption (2013); 19(2-4):501–508

[17] Watanabe M, Akimoto T, Kondoh E. Effects of surface modification of carbon nanotube on platinum nanoparticle deposition using supercritical carbon dioxide fluid. Phys. Status Solidi A 2012; 209(12):2514-2520

[18] Ziegler KJ, Gu Z, Peng H, Flor EL, Hauge RH, Smalley RE. Controlled Oxidative Cutting of Single-Walled Carbon Nanotubes. J Am Chem Soc 2005; 127(5):1541-1547

[19] Marshall MW, Popa-Nita S, Shapter JG; Measurement of functionalised carbon nanotube carboxylic acid groups using a simple chemical process. Carbon 2006; 44(7):1137–1141

[20] Forrest GA, Alexander AJ. A Model for the Dependence of Carbon Nanotube Length on Acid Oxidation Time. J Phys Chem C 2007; 111(29):10792-10798

[21] Yao N. Lordi V, Ma SXC. Dujardin E, Krishnan A, Treacy MMJ, et al. Structure and oxidation patterns of carbon nanotubes. J Mater Res 1998; 13(9)

[22] Rosca ID, Watari F, Uo M, Akasaka T. Oxidation of multiwalled carbon nanotubes by nitric acid. Carbon 2005; 43(15):3124–3131

[23] Zhang J, Zou H, Qing Q, Yang Y, Li Q, Liu Z, et al. Effect of Chemical Oxidation on the Structure of Single-Walled Carbon Nanotubes. J Phys Chem B 2003; 107(16):3712-3718

[24] Verdejo R, Lamoriniere S, Cottam B, Bismarck A, Shaffer M. Removal of oxidation debris from multi-walled carbon nanotubes. Chem Commun 2007; 5:513–515

[25] Fogden S, Verdejo R, Cottam B, Shaffer M. Purification of single walled carbon nanotubes: The problem with oxidation debris. Chem Phys Lett 2008; 460(1-3):162–167

[26] Stefani D, Paula AJ, Vaz BG, Silva RA, Andrade NF, Justo GZ. Structural and proactive safety aspects of oxidation debris from multiwalled carbon nanotubes. J Hazard Mater 2011; 189(1-2):391–396

[27] Wu Z, Hamilton RF Jr, Wang Z, Holian A, Mitra S. Oxidation debris in microwave functionalized carbon nanotubes: Chemical and biological effects. Carbon 2014; 68:678–686

[28] Wu Z, Mitra S. Microwave induced reactive base wash for the removal of oxidation debris from carboxylated carbon nanotubes. Carbon 2015; 88:233-238

[29] Kukovecz A, Konya Z, Nagaraju N,Willems I, Tamasi A, Fonseca A, et al. Catalytic synthesis of carbon nanotubes over Co, Fe and Ni containing conventional and sol–gel silica–aluminas. Phys Chem Chem Phys 2000; 2:3071-3076

[30] Gallagher PK, Gross ME. The thermal decomposition of palladium acetate. J Therm Anal 1986; 31:1231–1241

[31] Ajayan PM, Ebbesen TW, Ichihashi T, Iijima S, Tanigaki K, Hiura H. Opening carbon nanotubes with oxygen and implications for filling. Nature 1993; 362:522-525

[32] Dujardin E, Ebbesen TW, Krishnan A, Treacy MMJ. Purification of Single-Shell Nanotubes. Adv Mater 1998; 10(8):611-613

[33] Agnihotri S, Mota JPB, Rostam-Abadi M, Rood MJ. Adsorption site analysis of impurity embedded single-walled carbon nanotube bundles. Carbon 2006; 44(12):2376-2383

[34] Pushkarev VV, An K, Alayoglu S, Beaumont SK, Somorjai GA. Hydrogenation of benzene and toluene over size controlled Pt/SBA-15 catalysts: Elucidation of the Pt particle size effect on reaction kinetics. J Catal 2012; 292:64–72